ELSEVIER

Biophysical Chemistry 130 (2007) 17–25

Biophysical Chemistry

http://www.elsevier.com/locate/biophyschem

Solute effects on the irreversible aggregation of serum albumin

Heidi L. Bagger [a,c,1], Lars H. Øgendal [b], Peter Westh [a,*]

[a] Roskilde University, Department of Science, Models and Systems, Universitetsvej 1, DK-4000 Roskilde, Denmark
[b] University of Copenhagen, Department of Natural Sciences, Faculty of Life Sciences, Thorvaldsensvej 4, DK-1871 Frederiksberg C, Denmark
[c] Novozymes A/S, Kroghshøjvej 34, 2880 Bagsværd, Denmark

Received 15 April 2007; received in revised form 28 June 2007; accepted 28 June 2007
Available online 7 July 2007

Abstract

Thermal stress on bovine serum albumin (BSA) promotes protein aggregation through the formation of intermolecular β-sheets. We have used light scattering and chromatography to study effects of (<1 M) Na_2SO_4, NaSCN, sucrose, sorbitol and urea on the rate of the thermal aggregation. Both salts were strong inhibitors of BSA aggregation and they reduced both the size and number (concentration) of aggregate particles compared to non-ionic solutes (or pure buffer). Hence, the salts appear to suppress both nucleation- and growth rate. The non-electrolyte additives reduced the initial aggregation rate (compared to pure buffer), but did not significantly limit the extent of aggregation in samples quenched after 27 min. heat exposure (40–50% aggregation in all samples). The non-electrolytes did, however, modify the aggregation process as they consistently brought about smaller but more concentrated aggregates than pure buffer.

The results are discussed along the lines of linkage- and transition state theories. In this framework, the rate of the aggregation process is governed by the equilibrium between a thermally denatured state (D) and the transition state $D^{\neq}$. Thus, the effect of a solute relies on its preferential interactions with respectively D and $D^{\neq}$. The current results do not show any correlation between the solutes' preferential interactions with native BSA and their effect on the rate of aggregation. This suggests that non-specific, "Hofmeister-type" interactions, which scale with the solvent accessible surface area, are of minor importance. Rather, salt induced suppression of aggregation is suggested to depend on the modulation of specific electrostatic forces in the $D^{\neq}$ state.

Keywords: Multi angle light scattering; Size exclusion chromatography; Linkage theory; Transition state theory; Hofmeister series; Preferential interactions

1. Introduction

The physical instability of proteins in solution poses a major challenge for their technological and pharmaceutical utilization. One way of addressing this problem is to stabilize the protein's secondary and higher order structures through the addition of solutes such as certain sugars, polyols, salts and amino acids. For equilibrium processes, the way these changes in solvent composition modulates protein stability can be rationalized through the so-called Wyman relationships for linked equilibria [1]. One key aspect of this theory stipulates – along the lines of Le Chatelier's principle – that addition of a solute will favor the state with which it has the strongest (most favorable) interactions. More specifically the solute will change the equilibrium constant K for a denaturation equilibrium ($N \leftrightarrows D$) according to Eq. (1)

$$\left(\frac{\partial \ln K}{\partial \ln a_3}\right)_{T,P,a_2} = v_D - v_N = \Delta v \quad (1)$$

where a_3 is the thermodynamic activity of the solute. The function v is the preferential binding parameter, $v = (\partial m_3 / \partial m_2)_{T,P,a_3}$, where m_2 and m_3 denotes the molal concentration of respectively protein and solute. The preferential binding parameter can be experimentally assessed e.g. through dialysis equilibrium measurements, and this approach has been successful in attempts to understand solute effects on various protein equilibria [2–6]. In many cases, however, the loss of biological activity in protein

* Corresponding author. Fax: +45 4674 3011.
E-mail address: pwesth@ruc.dk (P. Westh).
[1] Current address: Ferring Pharmaceuticals, Kay Fiskers Plads 11, DK-2300 Copenhagen S, Denmark.

0301-4622/$ - see front matter © 2007 Elsevier B.V. All rights reserved.
doi:10.1016/j.bpc.2007.06.014

solutions does not progress reversibly, but relates to changes under kinetic control far from equilibrium. In these cases, it is challenging to establish a framework for the understanding of solute effects. However, one fundamental starting point, which has proven useful (for review see e.g. [7,8]), is the two-step molecular picture originally introduced by Lumry and Eyring [9].

$$N \leftrightarrows D \tag{2a}$$

$$D + A_n \rightarrow A_{n+1} \tag{2b}$$

The first step (Eq. (2a)) is an equilibrium transition ($\Delta G_{2a} \sim 0$) from the native (N) state to a non-native, aggregation competent conformation, D. The second (Eq. (2b)) is an irreversible growth step ($\Delta G_{2b} < 0$) in which the D state merges with a pre-established aggregate. Combining Eqs. (1), (2a) and (2b) suggests that solutes for which Δv is negative are likely to slow down the rate of aggregate formation since they displace the equilibrium (2a) towards the N state and thus lower the concentration of one "reactant" in (2b). Analogously, solutes which displace (2a) towards the right (i.e. $\Delta v > 0$ so that K is increased) may be expected to accelerate the observed rate of aggregation. This view suggests a direct correlation between the stabilization of N in (2a) and the kinetically controlled life-time of the active protein. Many reports have been in line with this interpretation both for stabilizing solutes such as sucrose ($\Delta v < 0$) and destabilizing solutes such as urea ($\Delta v > 0$) [7,10–15]. However, this strict coupling between equilibrium and kinetic stability is not universal and may be valid only at conditions where K is below or close to unity (i.e. when the N state is significantly populated) [16]. Moreover, the effects of solutes may be particularly complex as pointed out by Eronia et al. [11], who reported that additives which stabilized the N state of glucagon phosphorylase also promoted the rate of the protein's aggregation. Dual effects of solutes have also been reported for denaturants which promote aggregation and/or precipitation at low concentrations but inhibits it in somewhat more concentrated solutions [10,12,15]. One plausible interpretation of these dual effects is that the solute modulates the two steps in Eqs. (2a) and (2b) oppositely.

In the light of this, studies on possible interrelationships between preferential interactions and aggregation kinetics appear to be of interest. To this end we have investigated the effects of selected solutes (for which information on Δv and/or v_N is available) on the thermal aggregation of bovine serum albumin (BSA). To emphasize solute effects on the irreversible step (Eq. (2b)), we have studied the aggregation kinetics at the temperature T_d (determined separately by DSC), where the extent of reaction (2a) is 0.5 and hence $K = 1$ for all solutes (i.e. at slightly different temperatures for different types and concentration of solute). Hence, the initial D-concentration was expected to be equal in all trials. At neutral pH, the irreversible step for the thermal denaturation of BSA controlled by the formation of soluble "β-aggregates" in which a moderate part of the native helices are converted into intermolecular β-sheets which connect the protein monomers [17]. Under these conditions the aggregates are small, without pronounced polydispersity and their growth is governed by a reaction-limited mechanism [17–19]. These properties make BSA an adequate model system for studies of solute effects on irreversible transitions.

2. Methods

Albumin from bovine serum (BSA, >98%) was purchased from Sigma (St. Louis, USA). Prior to the experiments, BSA was dialyzed (MWCO 12–14 kDa), at 4 °C, against milliQ water and subsequently freeze dried. Sodium sulphate, Na_2SO_4, (>99.0%); sucrose (>99.5%) and sodium thiocyanate, NaSCN (>98%) were purchased from Fluka (Steinheim, Germany). Urea (>98%) and sorbitol (>98%) and succinic acid (>99%) was from Sigma. All solutions for calorimetry and light scattering measurements were prepared in 20 mM succinate buffer, pH 7.0. The freeze dried protein was quantified gravimetrically and dissolved in the succinic acid buffer to a stock solution with a protein concentration of 5.2 mg/ml. The investigated BSA samples were prepared by mixing this stock and solute–buffer mixtures to a final BSA concentration of 1.04 mg/ml.

Differential Scanning Calorimetry (DSC) was used to determine the denaturation temperature of BSA in the different solvents. The instrument was a SCAL-1 (Puschino, Russia). The protein solution was loaded into the sample cell (331 μl) and pure solvent into the reference cell. Both protein- and reference solution were degassed by stirring under vacuum prior to the experiment. The temperature was raised from 6 °C to 90 °C at a rate of 2 °C/minute under an excess pressure of 2 atm. The denaturation temperature, T_d, was defined at the maximum value of the heat capacity in the transition peak.

Static light scattering. The bulk aggregation kinetics of BSA was monitored in real time at the temperature T_d. We used a home built instrument for multi angle simultaneous static and dynamic light scattering [20]. The instrument uses a Nd–YAG laser (ADLAS325) with a wavelength of 532 nm and a power of 150 mW. The sample temperature is controlled to within 0.1 °C. For the current measurements, only the photon count rates recorded at 90° scattering angle were used.

Size exclusion chromatography with multi angle static light scattering and refractive index detection (SEC-MALLS) was used to characterize quenched samples. Aliquots of 500 μl were injected onto a 300 mm Superdex 200 column (Amersham Pharmacia) and eluded at 0.5 ml/min. The elution buffer was 50 mM NaH_2PO_4/Na_2HPO_4, pH 7.0, 15 mM NaCl. The species that eluted from the column were first passed through a light scattering instrument (DAWN EOS, Wyatt Technology, Santa Barbara, CA) equipped with a K2 flow cell, and subsequently through a differential refractometer (RID-10A, Shimadzu, Japan) for concentration determination. The light scattering instrument has 18 detectors that measure the intensity of the scattered light at different angles. In principle all but the detector corresponding to the smallest scattering angle are accessible with the K2 flow cell. In practice, however, a varying number of detectors both at the smallest and at the largest scattering angles have to be disregarded because the signal to noise ratio at the

Table 1
Experimental temperatures (T_d from the DSC trials) and slopes immediately after the lag period for the light scattering data in Fig. 1

	Sucrose		Urea		Sorbitol		Na_2SO_4		NaSCN		None
Conc. (M)	0.29	0.58	0.37	0.74	0.31	0.62	0.22	0.44	0.36	0.73	–
Exp. Temp. (°C)	69.5	70.0	67.5	67.0	69.0	70.0	68.5	68.5	74.0	72.0	68.5
$d(NSI_0)/dt \times 10^{-3}$	6.7	2.0	4.1	6.9	5.2	4.9	1.1	0.5	1.9	0.5	11.7

The slope is in s^{-1}.

extreme angles renders their signals useless. All chromatographic measurements were done at ambient temperature.

3. Results

3.1. Calorimetry

Variations in T_d were small. Thus, it increased 2 °C for sorbitol and sucrose over the concentration interval investigated here (0–0.6 M). A similar decrease was found for urea while no significant changes in T_d were detected for Na_2SO_4 (0–0.4 M). The only solute that produced distinctive effects was NaSCN which increased T_d by about 5 °C. This is highly unusual for this solute which is a strong chaotrope and accordingly commonly found to destabilize the native conformation [21]. However, an identical effect of thiocyanate on BSA has been reported before [22] and probably relates to a specific binding of the anion to native BSA. The values of T_d in all solvents, which were used as the experimental temperatures for the light scattering measurements, are listed in Table 1.

3.2. Static light scattering

The increase in the intensity of scattered light reflects the gradual aggregation of BSA in the sample. In the appendix we propose an approach for the analysis of the time course of the scattering. First, however, we plot (Fig. 1) the normalized scattering intensity, NSI as a function of time for the 11 different solvents. This function is defined as

$$NSI_t = (I_t - I_b)/I_0 \quad (3)$$

Where I is light intensity (in 90° scattering angle) and subscripts t, 0 and b identifies respectively a time dependent function, the value for $t=0$ and the background value for the protein-free solvent.

Fig. 1 shows that all trials share the common feature of a 2–3 min lag time in which no increase in NSI is observed. This behavior is typical to this type of measurements [8,17,23,24] and probably reflects the time required for thermal equilibration, equilibration of Eq. (2a) and nucleation of the aggregation process. Subsequent to the lag time, all solutes appear to inhibit thermal BSA aggregation as suggested directly from NSI values. This effect is particularly strong for the ionic solutes at the higher concentrations (>0.4 M). To get an estimate of the relative rates of aggregation, we determined the slope $dNSI/dt$ in the near-linear region (Fig. 1) just after the lag time. These values are listed in Table 1.

The distribution of monomers, dimers and aggregated proteins in the samples, which were quenched after 27 min at T_d, was investigated by SEC-MALLS. This method is particularly useful since the combined analysis of the RI and LS data provides information on the size and concentration of the aggregates even if they are too large to be resolved chromatographically. Fig. 2 shows examples of the SLS and RI signals from trials on both thermally denatured samples and samples which were kept refrigerated prior to the chromatography (referred to as reference samples). Panel A and B illustrate the effect of heat treatment of BSA in either pure buffer or 0.58 M sucrose. The RI signal (Fig. 2B) shows that in addition to the monomeric protein, the reference sample also contains a population (~14% w/w) of a species with twice the molecular weight (determined from the ASTRA software introduced below). This is most likely the Cys34 disulphide dimer, which is commonly found in BSA preparations [25]. The SLS profiles of reference samples, represented by bold lines in Fig. 2A, show four peaks corresponding to respectively aggregates (retention time 13–17 min), some smaller oligomers probably tri-, tetra and pentamers (20–22 min), dimers (22–25 min) and monomers (25–29 min). There was no significant difference between chromatograms (SLS and RI) of the eleven reference samples. The thin lines in Fig. 2A and B represent heat-treated samples of BSA in pure buffer (solid line) and in 0.58 M sucrose (dotted line). These results show a clear heat-induced increase in the

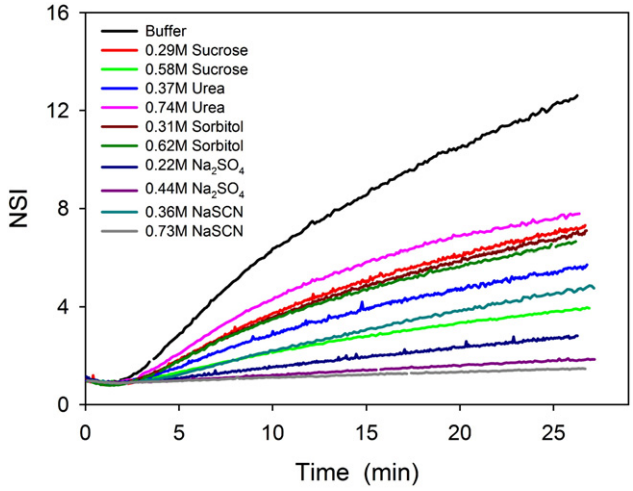

Fig. 1. Normalized scattering intensity, NSI, as a function of time for BSA (1.04 mg/ml) dissolved in 11 different solvents. pH was 7.0 in all samples. In black-and-white representations the curves are identified as (top-to-bottom at 25 min): Pure buffer, 0.74 M urea, 0.29 M sucrose, 0.31 M sorbitol, 0.62 M sorbitol, 0.37 M urea, 0.36 M NaSCN, 0.58 M sucrose, 0.22 M Na_2SO_4, 0.44 M Na_2SO_4, 0.73 M NaSCN.

amount of large aggregates and a concomitant decrease in the concentration of monomers and dimers. The chromatograms of all aggregated BSA solutions are shown in Fig. 2C and D. While present in the native samples, tetramers cannot be detected in the aggregated samples by either RI or SLS, and except the 0.73 M NaSCN solution, which shows a relative strong dimer peak (Fig. 2D), aggregation also seems to preferentially diminish the amount of dimers in all solutions. This enhanced tendency of oligomers to aggregate is in accord with the observation that BSA with a fluorophor covalently linked to cys-34 (preventing dimerization) exhibits reduced aggregation [19].

In general the aggregates are too large to be fully separated by this column, but their average molecular weight is reflected by the SLS data (Fig. 2C). Using the ASTRA software supplied with the SEC-MALLS instrument the average molecular weights of aggregates in the eleven different solvents were determined. The procedure for the evaluation of molecular weights deviated slightly from the recommend standard procedure for the DAWN light scattering instrument. First, baselines representing no light scattering or no RI signal are determined for all detectors. All subsequent calculations are then based on baseline corrected signals. The instrument has 18 LS detectors measuring the intensity of the scattered light at 18 different scattering angles, θ_1, θ_2,….., θ_{18}, but only detectors #9–14 (representing scattering angles 69.3°–121.2°) were used in the current analysis. The detectors do not have the same intrinsic sensitivity, so for each sample the central portion of the peak for the monomer (known to scatter isotropically) was used to normalize the detectors. This means that they should all yield the same signal as detector # 11 (90°) for the monomer peak after multiplication with individual correction factors k_j, j=9, 10,..., 14. Finally, an additional calibration factor, K_{cal}, common to all the detectors, is introduced. The value of this constant is determined by the requirement that the *apparent molecular weight* $M_{app}(\theta_j)$, i.e. one for each detector angle, calculated by the ASTRA software (Eq. (4)) all yield the correct molecular weight of the BSA monomer, 66.4 kD.

$$M_{app}(\theta_j) = K_{cal} \cdot k_j \cdot \frac{\sum_i LS_i(\theta_j)}{\sum_i RI_i} \text{ where } j = 9,10,\ldots,14 \qquad (4)$$

In this equation $LS_i(\theta_j)$ is the baseline corrected signal from the light scattering detector at scattering angle θ_j, and RI_i is the

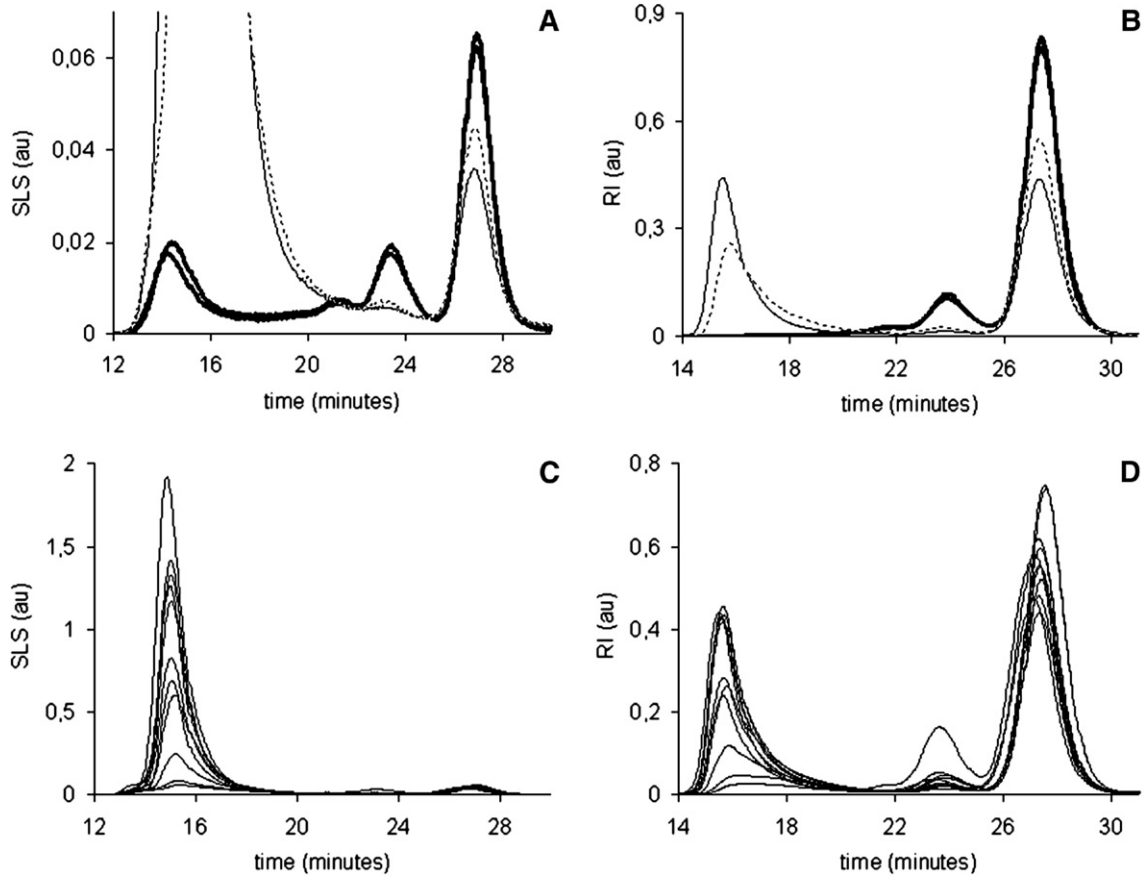

Fig. 2. Panel A and B show comparative chromatograms of heated (27 min at T_d) and not-heated (reference) BSA samples. The reference samples (in pure buffer and in 0.58 M sucrose) are represented by broad lines. The two chromatograms represented by thin lines in panel A and B refer to heated samples in respectively pure buffer (solid) and 0.58 M sucrose (dotted). Panel C and D show chromatograms of aggregated samples in the eleven investigated solvents. Left hand panels (A and C) represent data from the SLS detector (90° scattering angle). Right hand panels (B and D) represent data from the RI detector.

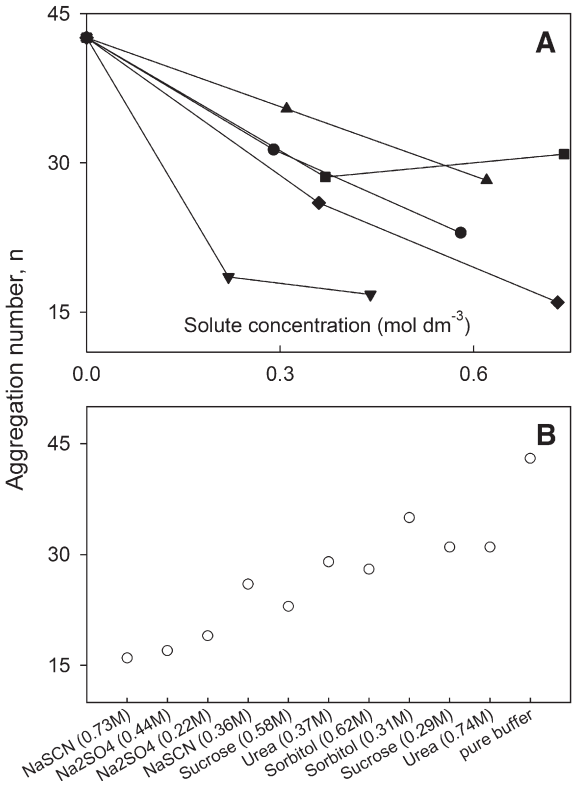

Fig. 3. The average number of BSA molecules, n, in the aggregates after 27 min of heat exposure. Panel A shows the dependence of n on the concentration of the solutes (down-triangles: Na_2SO_4, circles: sucrose, up-triangles: sorbitol, squares: urea and diamonds: NaSCN). In the histogram in panel B the solvents are organized with respect to initial aggregation rates (dNSI/dt) taken from Table 1.

signal from the refractometer. The index, i, in the sums has a range corresponding to the points constituting the monomer peak. In order to determine the molecular weight corresponding to the other peaks in the chromatograms Eq. (4) is again used to calculate the apparent molecular weights, where now the index i in the sums has a range corresponding to the peak whose molecular weight is being determined. The calibration constant K_{cal} and the normalization constants k_j have the values established by the procedure described above. The ASTRA program then determines the average molecular weight, M_w, by extrapolating the value of $M_{app}(\theta)$ to zero scattering angle using a Debye plot, i.e. assuming a linear relationship between $M_{app}(\theta)$ and $\sin^2\left(\frac{\theta}{2}\right)$.

For each peak in the chromatogram, specified by the range of the index variable i, the corresponding weight averaged molecular weight is determined using Eq. (3) followed by the extrapolation as described above. Results for the aggregate peak (retention time ~15 min) given as average aggregation numbers, $n = M_w/66.4$ kDa, are plotted as a function of the solute concentration in Fig. 3A. It appears that all investigated solutes bring about a decrease in the average aggregate size and that the ionic solutes, Na_2SO_4 and NaSCN, exert the strongest effect. The non-ionic polyols sucrose and sorbitol cause a linear decrease in n, while urea shows a minimum in Fig. 3A. In Fig. 3B, the solute systems are ranked according to their initial rate dNSI/dt (Table 1). This plot shows a gradual increase, which reveals that the aggregate size after 27 min. scales with the initial rate irrespectively of the chemical structure of the solute.

From a technological point of view, the most important parameter is not the aggregate size but the fraction of non-aggregated monomers (which may become biologically active if favorable conditions are reestablished). To elucidate this, we integrated the peaks in the RI chromatograms of respectively aggregated (Fig. 2D) and reference samples (bold lines in Fig. 2B). Before heat treatment the samples consisted of 82% (w/w) monomeric BSA, ~14% dimers, and ~4% higher order aggregates. The monomer peak decreased to different extends in different solvents upon heat treatment (Fig. 2) while the oligomers generally disappeared entirely. To illustrate this we calculated the mass fraction of BSA, f_A, which had become part of lager aggregates during the 27 min exposure to T_d.

The results in Fig. 4A and B show that Na_2SO_4 and NaSCN most effectively inhibit the thermally induced aggregation of BSA. For these solutes there is a clear correlation between the initial rates derived from real time light scattering and the fraction of BSA in aggregates in the quenched samples (Fig. 4B). For sorbitol, sucrose and urea, we find aggregation of 35–45% of the BSA, which is not significantly different from f_A in pure buffer. This suggests that in spite of the effects of these solutes on protein equilibria (sorbitol and sucrose as stabilizers, and urea as a denaturant) they exert little or no effect on the extent of BSA aggregation after 27 min.

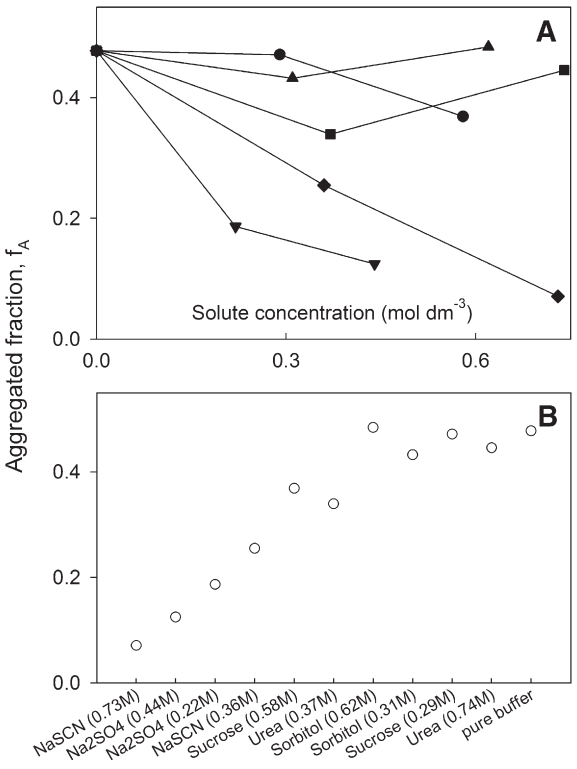

Fig. 4. Fraction of BSA, f_A, aggregated during the 27 min exposure to T_d. Panel A shows f_A as a function of the molar concentration of solute and panel B illustrates the relationship of f_A and the initial aggregation rate dNSI/dt. Symbols as in Fig. 3.

Having established the amount and average size of the aggregates in the quenched samples (Figs. 3 and 4), we estimated the concentration of aggregate particles, [A], according to Eq. (5),

$$[\mathrm{A}] = \frac{f_\mathrm{A} \cdot [\mathrm{BSA}]_\mathrm{tot}}{M_\mathrm{w}} \quad (5)$$

where $[\mathrm{BSA}]_\mathrm{tot}$ is the total amount of BSA (1.04 mg/ml or 16 μM). Fig. 5 shows that [A] is ~0.1–0.3 μM in the quenched samples, and that the ionic additives consistently decrease the particle concentration while the nonionic solutes have the opposite effect (Fig. 5A).

Taken together, Figs. 3–5 show that the ionic solutes are the strongest inhibitors of the investigated aggregation process — they induce both smaller and fewer BSA aggregates. In contrast, the non-electrolytes promote a higher concentration (Fig. 5) of smaller sized aggregates (Fig. 3), and thus exert limited effects of the overall degree of aggregation (Fig. 4).

3.3. Modeling of the real-time SLS

Above we have assessed the initial aggregation rates directly from the time course of the curves in Fig. 1 (subsequent to the lag time) by assuming proportionality of the scattered light intensity and the extent of aggregation. This approach has previously provided important insight into aggregation processes for other systems [8,11,12,23,24,26,27] but it is not unambiguous, for example because it neglects the fact that the intensity of the scattered light scales with the square of the molecular weight. To examine the consistency of the solvent-sequence used in Figs. 3B–5B, we derived an expression that correlated kinetic parameters and the intensity of the scattered light (see Appendix). The derivation was based on a number of approximations including the assumption of first order kinetics with respect to [D], constant particle concentration, [A], in the growth phase and rate limitation by the growth step, Eq. (2b). In general, non-linear regression by Eq. (A12) accounted well for the experimental data and Fig. 6 shows two representative examples. The kinetic parameter, k_2 (Eq. (A14)) derived from the regression analysis of the 11 solvents scaled with dNSI/dt, thus corroborating the sequence used in Figs. 3–5. We conclude that the initial slope in Fig. 1 may be used as a measure of the relative rate of aggregation in different solvents. The ratio k_2: dNSI/dt, however, was not constant and this calls for caution in the use of dNSI/dt as an absolute measure of the (first order) rate constant for thermal aggregation of BSA. A more detailed analysis of the relationship of slopes in plots like Fig. 1 and rate constants has been given elsewhere [8].

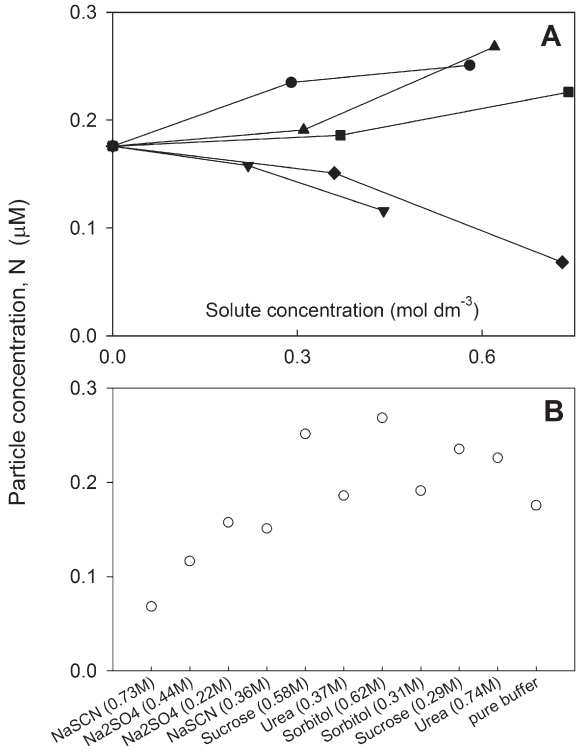

Fig. 5. Molar concentration of aggregate particles, [A], in the samples quenched after 27 min at T_d. Panel A shows [A] as a function of the molar concentration of solute and panel B illustrates the relationship of [A] and the initial aggregation rate dNSI/dt. Symbols as in Fig. 3.

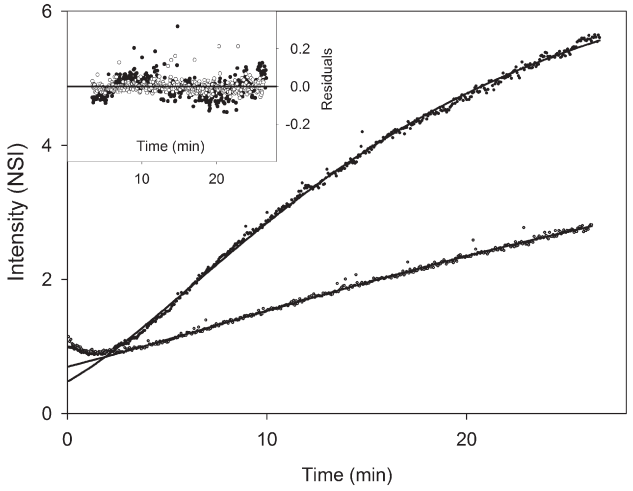

Fig. 6. Light scattering data for the thermal aggregation of BSA in respectively 0.27 M urea (upper curve) and 0.22 M Na_2SO_4 (lower curve). The dots are the experimental data and the solid lines are the regressions according to Eq. (A12) (see Appendix). The inset shows the residuals (urea: filled symbols, Na_2SO_4 open symbols). The first 3 min (i.e. the lag time) were neglected in the regression analysis.

4. Discussion

4.1. Aggregation mechanism and nucleation rate

Previous studies on thermal denaturation of BSA in pure buffer have suggested that the protein forms "soluble" aggregates in which a moderate fraction of the native α-helix is transformed into intermolecular β-sheet [17,19,28,29]. A similar trend has been found for numerous other proteins [30–32]. At pH values close to neutral, the aggregation of BSA is

reaction controlled whereas it becomes faster and diffusion controlled if pH is lowered towards pI, which is ~5 [17,18].

An initial lag time in light scattering data (Figs. 1 and 6) is typical for protein aggregation and reflects at least in part the nucleation process [23,33]. Accordingly, it has been suggested that the subsequent increase in scattering intensity is governed by the growth of embryo-aggregates formed during this lag period [8]. This simplification implies that the growth phase involves the adsorption of unfolded protein to a constant number of pre-established particles. The current data sheds some light on this, since the combined RI and MALLS analysis quantifies both the size (M_w) and concentration ([A]) of aggregate particles in the quenched samples. It appears that the salts decrease [A], while the non-ionic additives have the opposite effect (Fig. 5A). As all solutes decreased both the size of the aggregates after 27 min. (Fig. 3) and the initial aggregation rate (Table 1) one plausible interpretation is that the non-ionic additives promote the rate of nucleation in the lag phase, but retard the growth of particles at later stages. Hence, these solutions have a comparable large number of small aggregates. Addition of salts, on the other hand, inhibits both nucleation- and growth rates. This may suggest that although the BSA molecules carry the same net charge, nucleation and growth are both favored by electrostatic interactions, which are shielded by the ionic solutes.

4.2. Rate of aggregation

The pronounced effect of solutes on the rate of protein aggregation is illustrated in Table 1, which suggests that moderate concentrations (0.2–0.7 M) may change the initial rate of aggregation of BSA by more than an order of magnitude. To highlight the solute induced effect on the irreversible growth step (Eq. (2b)) all experiments were conducted at T_d, where the initial concentration of the D-form is (approximately) half of the total BSA concentration. One inevitable limitation of this experimental approach is the variation in experimental temperature. However, corrections using the Arrhenius equation and an activation energy of 300 kJ/mol [34] revealed only minor modifications. The largest changes were observed for 0.74 M urea, which increased to approximately the level of the pure buffer and thiocyanate which fell to around the values for sulfate. Comparisons of the initial rates (corrected or not) do not reveal any clear correlations to literature values of $\Delta\nu$ (Eq. (1)). For example, we did not find any significant difference between the stabilizer sorbitol ($\Delta\nu < 0$) and the denaturant urea ($\Delta\nu > 0$) [35–38] or between the two salt which are located in opposite ends of the Hofmeister series [39]. To examine this further we apply traditional transition state theory [40,41] for reaction controlled processes. If we assume that the irreversible step (Eq. (2B)) is rate limiting for the overall aggregation process we may expand Eq. (2a) to read.

$$N \leftrightarrows D \leftrightarrows D^{\neq} \rightarrow A \quad (6)$$

In Eq. (6), $D^{\neq}$ is the transition state or "activated complex". The observed rate of the aggregation process is proportional to the concentration of $D^{\neq}$, and the standard activation free energy of the process is $\Delta G^{\circ\neq} = -RT \cdot \ln K^{\neq}$, where R and T have their usual meanings and $K^{\neq}$ is the equilibrium constant $K^{\neq} = [D^{\neq}]/[D]$. The advantage of this approach is that the effect of a solute can be analyzed by equilibrium theory. Thus, solute effects on the second (rate determining) equilibrium in Eq. (6) may be expressed as $\partial \ln K^{\neq} / \partial \ln a_3 = \Delta\nu^{\neq}$, in complete analogy to Eq. (1). This approach thus stipulates that a solute's effect on the aggregation rate is governed by the difference of its preferential interaction with respectively the D and $D^{\neq}$ state ($\Delta\nu^{\neq}$). The pronounced inhibition of aggregation elicited by the two investigated salts thus implies negative (and rather similar) values of $\Delta\nu^{\neq}$. This consistency is interesting in the light of the disparity in their preferential interactions with typical proteins. Sulfate is a strong kosmotrope ($\nu_N < 0$) while thiocyanate is a strong chaotrope ($\nu_N > 0$) [21,42–44]. In many cases, the preferential binding parameter has been shown to be "non-specific" in the sense that it approximately scales with the solvent accessible surface area [4,38]. In such cases a preferentially excluded solute ($\nu_N < 0$) will displace any protein equilibrium towards the state with the lowest accessible area and *vice versa*. Since the two salts with different sign of ν_N act rather equally, we conclude that their effect on the thermal aggregation of BSA relies on specific interactions with the transition state (i.e. the preferential binding parameter is not proportional to the solvent accessible area). One likely interpretation is that the transition state is stabilized by electrostatic interactions, which are weakened by the ionic additive so that $\Delta G^{\circ\neq}$ increases with the salt concentration. Also, the results for the non-electrolytes suggest that the D- and $D^{\neq}$-states have similar solvent accessible areas, and consequently that $\Delta\nu^{\neq}$ will be close to zero for solutes interacting nonspecifically. This latter suggestion is in line with recent work by Rodriguez-Larrea et al. [45], who reported modest changes in the solvent accessibility of the transition state during the irreversible denaturation of a lipase. The limited importance of non-specific interactions is also emphasized by the rather constant extend of aggregation (Fig. 4) in samples with respectively sorbitol, sucrose and urea.

In closing we suggest that the combined use of linkage- and transition state theories offers a promising approach for systematic analysis and comparison of solute effects on protein aggregation rates — an area of considerable interest in biotechnology. Related suggestions has previously been put forward [7,46]. The current results show that for BSA, the lyotropic properties of a solute (reflected in its position in the Hofmeister series [39]) are of minor importance both for the rate of the irreversible step and for the size and concentration of aggregate particles in heat-treated samples.

Acknowledgements

This work was supported by Novozymes A/S through the establishment of the "Protein Stability Network". Financial support by the Carlsberg Foundation, Danish Research Agency (grants 26-02-0160 and 21-04-0087 to PW) and the Ministry of Science Technology and Innovation is gratefully acknowledged.

Appendix A

In order to interpret the bulk SLS data a model for the aggregation and the resulting intensity of the scattered light is needed. We take as a starting point, the Lumry and Eyring model mentioned in the introduction

$$\mathrm{N} \leftrightarrows \mathrm{D}, K = \frac{[\mathrm{D}]}{[\mathrm{N}]} \tag{A1}$$

$$\mathrm{D} + \mathrm{A}_n \rightarrow \mathrm{A}_{n+1} \tag{A2}$$

We will assume that the formation of aggregates proceeds through the formation of nucleation species, seeds, with a concentration [A]. All subsequent aggregation proceeds by addition of denatured protein monomer to already existing aggregates. Thus, the number of aggregates remains constant and equal to [A]. The aggregation process is assumed to be first order in the sense that

$$\frac{\mathrm{d}n}{\mathrm{d}t} = k_2 \cdot [\mathrm{D}] \tag{A3}$$

where k_2 is a rate constant (unit $\mathrm{M}^{-1}\cdot\mathrm{s}^{-1}$). Throughout the aggregation process mass is conserved which can be expressed as

$$[\mathrm{N}] + [\mathrm{D}] + n \cdot [\mathrm{A}] = c_0 \tag{A4}$$

where c_0 is the molar concentration of added protein when the solution is prepared. We now make a differential equation for [D] by first differentiating and next rearranging Eq. (A4) giving

$$\frac{dn}{dt} = -\frac{1}{[\mathrm{A}]} \cdot \frac{\mathrm{d}([\mathrm{N}] + [\mathrm{D}])}{\mathrm{d}t} \tag{A5}$$

If the Equilibrium (A1) is fast enough that the native and denatured protein molecules remain in equilibrium while aggregation proceeds then Eq. (A5) can be combined with Eq. (A3) to give the differential equation

$$\frac{d[\mathrm{D}]}{dt} = -\frac{k_2[\mathrm{A}]}{1 + 1/K} \cdot [\mathrm{D}] \tag{A6}$$

having the general solution

$$[\mathrm{D}] = D_0 \cdot e^{-\lambda \cdot t} \tag{A7}$$

where

$$\lambda = k_2[\mathrm{A}]/(1 + 1/K) \tag{A8}$$

At infinite times no denatured or native protein is left and the all monomers are bound in aggregates with the aggregation number

$$n_{\max} = \frac{c_0}{[\mathrm{A}]} \tag{A9}$$

Particles in solution scatter light in proportion to their molar concentration and the square of their molecular weight. Therefore the intensity of scattered light of the aggregating solution can be written as

$$I_{\mathrm{scat}} = k_{\mathrm{scat}} \cdot \left([\mathrm{N}] + [\mathrm{D}] + n^2[\mathrm{A}]\right) = k_{\mathrm{scat}} \cdot \left((1 + 1/K)[\mathrm{D}] + n^2[\mathrm{A}]\right) \tag{A10}$$

where k_{scat} is a constant depending on instrumental details as well as properties of the investigated system but not on the aggregation state of the protein. Solving Eq. (A4) for n and using Eq. (A7) the scattered intensity (A10) can be written

$$I_{\mathrm{scat}} = k_{\mathrm{scat}} \cdot \left((1 + 1/K)D_0 \cdot e^{-\lambda \cdot t} + \left(c_0 - (1 + 1/K)D_0 \cdot \mathrm{e}^{-\lambda \cdot t}\right)^2 / S_0\right) \tag{A11}$$

If the parameter $\lambda_0 = k_2 D_0$ is introduced Eq. (A11) can be rewritten

$$I_{\mathrm{scat}} = I_0 \cdot \left(\frac{\lambda_0}{\lambda \cdot n_{\max}} \cdot e^{-\lambda \cdot t} + n_{\max} \cdot \left(1 - \frac{\lambda_0}{\lambda \cdot n_{\max}} \cdot \mathrm{e}^{-\lambda \cdot t}\right)^2\right) \tag{A12}$$

This expression can be fitted to the bulk scattering data through adjustment of the free parameters I_0, λ_0, λ and $n_{\max}$. Notice that the expression works equally well with normalized and non-normalized scattering data.

Although not evident from the mathematical structure of the fitting expression (A12) it turns out that the parameter $n_{\max}$ correlates strongly with the other parameters. This problem can be circumvented because both the weight fraction f in the aggregated state and the value of the aggregation number $n(t_0)$ has been determined in the SEC-MALLS experiments at time $t_0 = 6120$ s = 27 min. Still assuming that all aggregation after t_0 only increases the aggregation number (and not molar concentration of the aggregates) it is seen that

$$n_{\max} = \frac{n(t_0)}{f} \tag{A13}$$

which can be added as a constraint on Eq. (A12) while fitting.

When the fitting parameters have been determined, the physical parameters can be calculated using $K = 1$. Since the measurements were done at T_{m}, $[A] = \frac{c_0}{n_{\max}}$, and

$$k_2 = \frac{2\lambda n_{\max}}{c_0} \tag{A14}$$

References

[1] J.G. Wyman, S.J. Gill, Binding and Linkage, Functional Chemistry of Biological molecules, University Science Books, Mill Valley, CA, 1990.
[2] P.R. Davis-Searles, A.J. Saunders, D.A. Erie, D.J. Winzor, G.J. Pielak, Interpreting the effects of small uncharged solutes on protein-folding equilibria, Annu. Rev. Biophys. Biomol. Struct. 30 (2001) 271–306.

[3] S.N. Timasheff, Protein–solvent preferential interactions, protein hydration, and the modulation of biochemical reactions by solvent components, Proc. Natl. Acad. Sci. U.S.A. 99 (2002) 9721–9726.
[4] S.N. Timasheff, Control of protein stability and reactions by weakly interacting cosolvents: The simplicity of the complicated, Adv. Protein Chem. 51 (1998) 355–432.
[5] T. Arakawa, S.N. Timasheff, Theory of protein solubility, Methods Enzymol. 114 (1985) 49–77.
[6] M.T. Record, W.T. Zhang, C.F. Anderson, Analysis of effects of salts and uncharged solutes on protein and nucleic acid equilibria and processes: a practical guide to recognizing and interpreting polyelectrolyte effects, Hofmeister effects, and osmotic effects of salts, Adv. Protein Chem. 51 (1998) 281–353.
[7] E.Y. Chi, S. Krishnan, T.W. Randolph, J.F. Carpenter, Physical stability of proteins in aqueous solution: Mechanism and driving forces in nonnative protein aggregation, Pharm. Res. 20 (2003) 1325–1336.
[8] B.I. Kurganov, Kinetics of protein aggregation. Quantitative estimation of the chaperone like activity in test systems based on suppression of protein aggregation, Biochem. (Moscow) 67 (2002) 409–422.
[9] R. Lumry, H. Eyring, Conformation changes of proteins, J. Phys. Chem. 58 (1954) 110–120.
[10] L.R. DeYoung, K.A. Dill, A.L. Fink, Aggregation and denaturation of apomyoglobin in aqueous urea solutions, Biochem. 32 (1993) 3877–3886.
[11] T.B. Eronina, N.A. Chebotareva, B.I. Kurganov, Influence of osmolytes on inactivation and aggregation of muscle glycogen phosphorylase b by guanidine hydrochloride. Stimulation of protein aggregation under crowding conditions, Biochem.-Moscow 70 (2005) 1020–1026.
[12] T.B. Eronina, N.A. Chebotareva, N.B. Livanova, B.I. Kurganov, Kinetics of denaturation of rabbit skeletal muscle glycogen phosphorylase b by guanidine hydrochloride, Biochem.-Moscow 66 (2001) 449–455.
[13] B.S. Kendrick, J.F. Carpenter, J.L. Cleland, T.W. Randolph, A transient expansion of the native state precedes aggregation of recombinant human interferon-gamma, Proc. Natl. Acad. Sci. U.S.A. 95 (1998) 14142–14146.
[14] B.A. Kerwin, M.C. Heller, S.H. Levin, T.W. Randolph, Effects of Tween 80 and sucrose on acute short-term stability and long-term storage at −20 degrees C of a recombinant hemoglobin, J. Pharm. Sci. 87 (1998) 1062–1068.
[15] Y.S. Kim, S.P. Cape, E. Chi, R. Raffen, P. Wilkins-Stevens, F.J. Stevens, M.C. Manning, T.W. Randolph, A. Solomon, J.F. Carpenter, Counteracting effects of renal solutes on amyloid fibril formation by immunoglobulin light chains, J. Biol. Chem. 276 (2001) 1626–1633.
[16] S.E. Zale, A.M. Klibanov, On the role of reversible denaturation (unfolding) in the irreversible thermal inactivation of enzymes, Biotechnol. Bioeng. 25 (1983) 2221–2230.
[17] V. Militello, C. Casarino, A. Emanuele, A. Giostra, F. Pullara, M. Leone, Aggregation kinetics of bovine serum albumin studied by FTIR spectroscopy and light scattering, Biophys. Chemist. 107 (2004) 175–187.
[18] T. Hagiwara, H. Kumagai, K. Nakamura, Fractal analysis of aggregates formed by heating dilute BSA solutions using light scattering methods, Biosci. Biotechnol. Biochem. 60 (1996) 1757–1763.
[19] V. Militello, V. Vetri, M. Leone, Conformational changes involved in thermal aggregation processes of bovine serum albumin, Biophys. Chemist. 105 (2003) 133–141.
[20] R. Bauer, M. Hansen, S. Hansen, L. Ogendal, S. Lomholt, K. Qvist, D. Harne, The structure of casein aggregates during renneting studied by indirect fourier transformation and inverse Laplace transformation of static and dynamic light-scattering data, respectively, J. Chem. Phys. 103 (1995) 2725–2737.
[21] K.D. Collins, M.W. Washabaugh, The Hofmeister effect and the behavior of water at interfaces, Q. Rev. Biophys. 18 (1985) 323–422.
[22] M. Yamasaki, H. Yano, K. Aoki, Differential scanning calorimetric studies on bovine serum albumin: II. Effects of neutral salts and urea, Int. J. Biol. Macromol. 13 (1991) 322–328.
[23] N.V. Fedurkina, L.V. Belousova, L.G. Mitskevich, H.M. Zhou, Z. Chang, B.I. Kurganov, Change in kinetic regime of protein aggregation with temperature increase. Thermal aggregation of rabbit muscle creatine kinase, Biochem.-Moscow 71 (2006) 325–331.
[24] R. Hoiberg-Nielsen, C.C. Fuglsang, L. Arleth, P. Westh, Interrelationships of glycosylation and aggregation kinetics for *Peniophora lycii* phytase, Biochem. 45 (2006) 5057–5066.
[25] T. Peters, Serum-albumin, Adv. Protein Chem. 37 (1985) 161–245.
[26] B.I. Kurganov, E.R. Rafikova, E.N. Dobrov, Kinetics of thermal aggregation of tobacco mosaic virus coat protein, Biochem.-Moscow 67 (2002) 525–533.
[27] J.M. Finke, M. Roy, B.H. Zimm, P.A. Jennings, Aggregation events occur prior to stable intermediate formation during refolding of interleukin 1 beta, Biochem. 39 (2000) 575–583.
[28] A.H. Clark, D.H.P. Saunderson, A. Suggett, Infrared and laser-Raman spectroscopic studies of thermally-induced globular protein gels, Int. J. Pept. Protein Res. 17 (1981) 353–364.
[29] A.H. Clark, C.D. Tuffnell, Small-angle X-ray-scattering studies of thermally-induced globular protein gels, Int. J. Pept. Protein Res. 16 (1980) 339–351.
[30] A.L. Fink, Protein aggregation: folding aggregates, inclusion bodies and amyloid, Fold. Des. 3 (1998) R9–R23.
[31] B.S. Kendrick, J.L. Cleland, X. Lam, T. Nguyen, T.W. Randolph, M.C. Manning, J.F. Carpenter, Aggregation of recombinant human interferon gamma: Kinetics and structural transitions, J. Pharm. Sci. 87 (1998) 1069–1076.
[32] D. Thirumalai, D.K. Klimov, R.I. Dima, Emerging ideas on the molecular basis of protein and peptide aggregation, Curr. Opin. Struck. Biol. 13 (2003) 146–159.
[33] B.I. Kurganov, Kinetics of protein aggregation. Quantitative estimation of the chaperone-like activity in test-systems based on suppression of protein aggregation, Biochem.-Moscow 67 (2002) 409–422.
[34] S. Baier, J. McClements, Impact of preferential interactions on thermal stability and gelation of bovine serum albumin in aqueous sucrose solutions, J. Agric. Food Chem. 49 (2001) 2600–2608.
[35] J.K. Kaushik, R. Bhat, Thermal stability of proteins in aqueous polyol solutions: Role of the surface tension of water in the stabilizing effect of polyols, J. Phys. Chem., B 102 (1998) 7058–7066.
[36] H. Uedaira, H. Uedaira, The effect of sugars on the thermal-denaturation of lysozyme, Bull. Chem. Soc. Jpn. 53 (1980) 2451–2455.
[37] J.F. Back, D. Oakenfull, M.B. Smith, Increased thermal-stability of proteins in the presence of sugars and polyols, Biochem. 18 (1979) 5191–5196.
[38] E.S. Courtenay, M.W. Capp, C.F. Anderson, M.T. Record Jr., Vapor pressure osmometry studies of osmolyte–protein interactions: implications for the action of osmoprotectants in vivo and for the interpretation of "osmotic stress" experiments in vitro, Biochem. 39 (2000) 4455–4471.
[39] K.D. Collins, M.W. Washabaugh, The Hofmeister effect and the behaviour of water at interfaces, Q. Rev. Biophys. 18 (1985) 323–422.
[40] H. Eyring, The activated complex in chemical reactions, J. Chem. Phys 3 (1935) 107–115.
[41] J.E. House, Principles of chemical kinetics, W.C. Brown Editors, Dubuque, IA, 1990.
[42] T. Arakawa, S.N. Timasheff, Preferential interactions of proteins with salts in concentrated-solutions, Biochem. 21 (1982) 6545–6552.
[43] T. Arakawa, S.N. Timasheff, Protein stabilization and destabilization by guanidinium salts, Biochem. 23 (1984) 5924–5929.
[44] T. Arakawa, S.N. Timasheff, Mechanism of protein salting in and salting out by divalent-cation salts — balance between hydration and salt binding, Biochem. 23 (1984) 5912–5923.
[45] D. Rodriguez-Larrea, S. Minning, T.V. Borchert, J.M. Sanchez-Ruiz, Role of solvation barriers in protein kinetic stability, J. Mol. Biol. 360 (2006) 715–724.
[46] B.M. Baynes, B.L. Trout, Rational design of solution additives for the prevention of protein aggregation, Biophys. J. 87 (2004) 1631–1639.